OPG-Fc inhibits ovariectomy-induced growth of disseminated breast cancer cells in bone

Penelope D Ottewell[1], Ning Wang [2], Hannah K Brown[1], C Anne Fowles[2], Peter I Croucher[3], Colby L Eaton[2] and Ingunn Holen[1]

[1]Academic Unit of Clinical Oncology, Department of Oncology, [2] Academic Unit of Bone Biology, Department of Human Metabolism, University of Sheffield, S10 2RX, UK and [3]Musculoskeletal Medicine Division, Garvan Institute of medical Research, Sidney, New South Wales, Australia.

Corresponding author: Dr. Penelope Ottewell, Academic Unit of Clinical Oncology, Medical School, University of Sheffield, Beech Hill Road, Sheffield, S10 2RX, UK.

Telephone: +44 (0) 114 271 2133

Fax: +44 (0) 114 271 1711

E-Mail : p.d.ottewell@sheffield.ac.uk

Key Words : Breast Cancer, OPG, Metastasis, Bone

Short title : OPG-Fc inhibits breast cancer bone metastasis

Abstract

Background: Dormant disseminated tumour cells can be detected in the bone marrow of breast cancer patients several years after resection of the primary tumour. The majority of these patients will remain asymptomatic, however, ~15% will go on to develop overt bone metastases and this condition is currently incurable. The reason why these dormant cells are stimulated to proliferate and form bone tumours in some patients and not others remains to be elucidated. We have recently shown that in an *in vivo* model, increasing bone turnover by ovariectomy stimulated proliferation of disseminated tumour cells, resulting in formation of bone metastasis. We now show for the first time that osteoclast mediated mechanisms induce growth of tumours from dormant MDA-MB-231 cells disseminated in the bone. We also show that disruption of RANK-RANKL interactions following administration of OPG-Fc inhibits growth of these dormant tumour cells *in vivo.* Our data support early intervention with anti-resorptive therapy in a low-oestrogen environment to prevent development of bone metastases.

Introduction

Metastatic breast cancer remains a considerable clinical challenge, causing around 12,000 deaths annually in the UK alone. The majority of patients with advanced disease will develop bone metastases, in many cases several years after removal of the primary tumour. It is increasingly accepted that, in breast cancer, the dissemination of tumour cells from the primary site to specific niches in the bone marrow is an early event, completed prior to diagnosis and initiation of therapy. Tumour cells can remain dormant in the bone marrow for decades and may never proliferate to form overt bone metastases. The precise cellular and molecular mechanisms that regulate tumour cell dormancy in bone, and the signals that trigger tumour cell escape from dormancy, remain to be established. However, the tumour microenvironment is suggested to play a major role in both processes, and therefore represents a key therapeutic target (1-2).

Development and progression of breast cancer bone metastases has been intensely studied, demonstrating that the process is driven by close interactions between tumour cells and components of the bone microenvironment. In particular, tumour cell-mediated stimulation of the bone-resorbing osteoclasts is shown to be responsible for the lytic bone lesions associated with late stage disease (3). In contrast, our understanding of the early stages of tumour cell dissemination to the skeleton, as well as the initiation of tumour cell growth, is less clearly defined. Both osteoblasts and osteoclasts, as well as components of the extracellular matrix, are proposed to play a role in the early stages of bone metastasis (reviewed in: 3,4).

Due to the key role of the bone microenvironment, treatment of overt bone metastases involves a combination of agents that target tumour cells directly as well as bone-targeted agents like bisphosphonates and denosumab (5,6). However, whether adjuvant targeting of the bone microenvironment (in particular the osteoclast) can reduce bone metastasis remains controversial. The recently published AZURE trial found that treating breast cancer patients considered at high risk of developing bone metastases with Zoledronic acid was only beneficial in patients with established menopause (7). This surprising result has been confirmed in other clinical trials, but the underlying mechanisms are yet to be identified. Adjuvant trials of denosumab are ongoing (D-CARE), and will provide further information as to whether osteoclast-mediated processes are key to the differential effects on breast cancer bone metastasis according to menopausal status.

One of the main unanswered questions in relation to initiation of bone metastasis is how changes to the bone microenvironment, including accelerated bone turnover, affects disseminated tumour cells in bone. Recent advances in technology have facilitated the studies of individual tumour cells within their resident bone niches. We and others have used a combination of *in vivo* bone metastasis models and advanced imaging to investigate how bone-targeted agents modify the bone microenvironment and how this affects subsequent tumour cell homing/proliferation (8-12,). Using this approach, we recently demonstrated that accelerated bone turnover caused by ovariectomy (OVX) resulted in proliferation of disseminated tumour cells and increased levels of bone metastases (8). Tumour growth in bone was inhibited by the anti-resorptive agent zoledronic acid, suggesting that osteoclast activity is involved in regulating early stages of bone metastasis, as well as in end stage disease. If this hypothesis is correct, other anti-resorptive agents working through different mechanisms should also prevent both OVX-induced bone loss and growth of dormant tumour cells in bone. The agent of choice to investigate this is denosumab, a monoclonal antibody that binds human receptor activator of nuclear factor (NF)-kB ligand (RANKL) with high affinity, thereby blocking RANK-RANKL interactions essential for osteoclastogenesis. Denosumab is shown to be superior to zoledronic acid for the prevention or delay of skeletal complications in patients with advanced cancer and bone metastases (13). However, denosumab is human specific and cannot be used in murine *in vivo* models. Instead we have used OPG-Fc, a potent inhibitor osteoclastogenesis that acts by preventing RANKL-RANK binding and hence modifies the same pathways as denosumab (14). We investigated the effects of inhibiting OVX-induced bone resorption through targeting RANKL-RANK interactions in an *in vivo* model of disseminated breast cancer cells in bone.

The current study is the first to demonstrate that administration of OPG-Fc inhibits OVX-induced growth of disseminated, dormant, tumour cells in bone *in vivo.* Our data support the early administration of anti-resorptive therapy in a low-oestrogen setting to prevent development of bone metastases.

Materials and methods

Cell Culture: Low passage (< P10) human MDA-MB-231 breast cancer cells transfected with the red fluorescent protein, TdTomato (RFP) and second generation luciferase (luc-2) (Calliper Life Sciences, Manchester, UK) were cultured in DMEM + 10% FCS (Gibco®, Invitrogen, Paisley, UK). Prior to injection, tumour cells were incubated for 15 minutes with 25μM of 1,1'-Dioctadecyl-', 3'-Tetramethylindodicarbocyanine, 4-Chlorobenzenesulfonate (DiD) (Life Technologies, Paisley, UK). DiD is a lipophilic membrane dye that becomes diluted each time the cell divides enabling visualisation of non-proliferating, disseminated tumour cells in bone by 2-photon microscopy. Tumour growth was monitored using an IVIS Lumina II system (Calliper Life Sciences).

***In vitro* experiments:** For cell proliferation experiments, $1x10^4$ MDA-MB-231 cells were seeded in 2mls of DMEM + 0, 2.5, 5, 7.5 or 10% FCS in 12 well tissue culture plates (Corning, Paisley, UK). 24h after seeding cells were treated with 0, 10, 50 or 100μg/ml recombinant OPG (OPG-Fc) (comprising amino acids 22-194 of human OPG fused at the N-terminus of the Fc domain of human immunoglobulin G1 (15). This compound is certified as endotoxin free and was a kind gift from Amgen). Cells were harvested using trypsin/EDTA (SigmaAldrich, Poole, UK) at 24, 48, 72 and 144h and numbers of tumour cells were counted using a hemacytometer. For clonogenic assays 1000 or 500 cells were seeded into 6-well tissue culture plates containing saline / 100μg/ml OPG-Fc in 2mls DMEM or into 2mls of DMEM and left for 24h before addition of OPG-Fc. All experiments were carried out three times in triplicate

***In vivo* studies:** We used 12-week-old female BALB/c nude mice (Charles River, Kent, UK). Experiments were carried out in accordance with local guidelines and with Home Office approval under project licence 40/3462, University of Sheffield, UK.

To investigate the effects of ovariectomy on dormant tumour cells in bone, $1x10^5$ MDA-MB-231 cells were injected into the left cardiac ventricle of 19 mice. Mice were ovariectomised or sham ovariectomised (n=7/group) 56 days after tumour cell injection and culled 28 days later. In addition, 5 mice were culled on day 56 and analysed for presence of disseminated tumour cells in the long bones.

Effects of OPG-Fc on bones were analysed 4 weeks following weekly intra-venous injection (i.v) of 25mg/kg OPG-Fc. Effects of OPG-Fc on ovariectomy-induced tumour growth were investigated in mice injected into the left cardiac ventricle with $1x10^5$ DiD labelled MDA-MB-231 cells on day 0. On day 5 mice were given weekly OPG-Fc (25mg/kg i.v) or saline (n=20/group) and on day 7, animals from both groups underwent either sham or ovariectomy (n=7/group).

Whole blood was collected by cardiac puncture and the isolated serum was stored at -80^0C for ELISA, tibiae and femurs were fixed in 4% PFA for μCT analysis before decalcification in 1%PFA/0.5% EDTA and processing for histology. Bones for two-photon analysis were stored in OCT at -80^0C.

Microcomputed tomography imaging: Microcomputed tomography analysis was carried out using a Skyscan 1172 x-ray-computed microtomography scanner (Skyscan, Aartselaar, Belgium) equipped with an x-ray tube (voltage, 49kV; current, 200uA) and a 0.5-mm aluminium filter was used. Pixel size was set to 5.86 μm and scanning initiated from the top of the proximal tibia as previously described (16).

Bone histology: Histological sections (5μM) of decalcified tibiae (5μmol/L EDTA fro 4 weeks) were stained with Goldner's trichrome or Safranin O using standard protocols. Osteoclasts were detected by tartrate-resistant acid phosphatase (TRAP) staining and osteoblasts were identified as mononuclear, cuboidal cells residing in chains along the bone surface as previously described (17).

Two-photon microscopy: Detection of individual tumour cells disseminated into mouse tibiae in which no tumour growth was observed by luciferase imaging was carried out by two-photon microscopy. Dissected tibias were snap frozen in liquid nitrogen, embedded in CryoMBed embedding medium and trimmed longitudinally to expose bone marrow area using a cryostat (Bright 126 Instrument Co. Ltd). A stack area of 2104μm (X) x 2525μm (Y) x 100μm (Z) incorporating the proximal tibiae was imaged (Zeiss LSM510 NLO microscope Carl Zeiss Inl). DiD labelled, non-proliferating, tumour cells were visualised using a 633nm

Chameleon laser, bone was detected using the 900nm multiphoton laser (Coherent, Santa Clara, CA.) and images were reconstructed in LSM software version 4.2 (Zeiss).

Biochemical analysis: Serum concentrations of TRAP 5b and P1NP were measured using commercially available ELISA kits: MouseTRAP™ Assay (Immunodiagnostic systems) and Rat/Mouse P1NP competitive immunoassay kit (Immunodiagnostic Systems), respectively.

Statistical Analysis: Statistical analysis was by one way analysis of variance (ANOVA) followed by Newman-Keuls multiple comparison test. Statistical significance was defined as P less than or equal to 0.01. All P values are two-sided.

Results

Effects of ovariectomy on growth of dormant breast cancer cells in bone

We have previously shown that ovariectomy (OVX) increases bone turnover in 12-week old mice and that performing OVX, either 7 days before or 7 days after intra-cardiac (i.c.) injection of breast cancer cells, results in significantly increased bone metastasis (8). To more closely mimic the clinical situation, where disseminated tumour cells lie dormant in bone for prolonged periods, we have now investigated whether OVX also induces growth of tumour cells that have remained non-proliferative in bone for 8 weeks. BALB/c nude mice were injected i.c. with MDA-MB-231 cells on day 0 and monitored by weekly *in vivo* imaging. If animals had not developed long bone metastases by day 56, the disseminated tumour cells in bone were considered to be dormant. Animals without long bone tumours underwent either OVX (n=7) or sham operation (n=7) on day 56. A cohort of animals was culled to confirm the presence of dormant disseminated tumour cells in long bones (n=5) (figure 1a).

As expected, OVX stimulated tumour growth in the long bones, with bone metastases detected in 6/7 mice 4 weeks later (figure 1b). In contrast, no metastases were seen in the long bones of sham operated animals. Tumour growth at other sites, including spine, ribs and head, were comparable in both experimental groups and was unaltered by ovariectomy (figure 1c). Analysis of tibiae 56 days following tumour cell injection confirmed the presence of non-proliferating (dormant) DiD-labelled cells in close proximity to trabecular bone (figure 1d). DiD-labelled tumour cells were detected in the tibia of all mice, including those that did not develop tumours by the end of the experimental protocol (day 84). µCT analysis of proximal tibiae from OVX and sham operated mice confirmed that OVX significantly reduced trabecular bone volume compared with tissue volume $P < 0.01$ (figure 1 e).

These data demonstrate that tumour cells can remain dormant in bone for prolonged periods of time *in vivo*, and that altering the bone microenvironment through OVX triggers their proliferation and development into overt bone metastases.

Effects of OPG-Fc on the bone microenvironment

We next investigated whether the OVX-induced changes to the bone microenvironment could be counteracted by inhibition of bone turnover. Osteoprotegerin (OPG) inhibits

osteoclastogenesis through disrupting RANKL-RANK interactions (14). We established the effects of weekly administration of 25mg/kg OPG-Fc on the bone microenvironment in our model system. As shown in figure 2, animals receiving OPG-Fc displayed increased bone volume, had an extended growth plate and reduced serum levels of markers of both osteoclast (TRAP) and osteoblast (P1NP) activity, compared to the control group. This was accompanied by striking reductions in the numbers of osteoblasts and osteoclasts (figure 2a). Scoring of histological sections revealed 3.22 ± 1.46 osteoclasts and 98.16 ± 17.42 osteoblasts per mm of bone surface in tibiae of control mice, whereas both cell types were undetectable on endocortical and trabecular surfaces of tibiae 4 weeks following weekly injection of 25mg/kg OPG-Fc. The most dramatic change was seen in the bone volume, with the percentage of bone volume compared with tissue volume increasing from 8.19 ± 0.29% in control animals to 23.55 ± 0.21% in animals receiving OPG-Fc, $p < 0.001$. This change was mainly due to the extended growth plate and increased proteoglycan rich matrix in the metaphysis of bones from OPG-Fc treated compared with control mice (figure 2a). The increase in bone volume may, therefore, be a result of elevated ossification due OPG-Fc induced disruption of osteoclast activity preventing resorption of this access matrix.

OPG-Fc inhibits OVX-induced growth of disseminated tumour cells

Having established that OPG-Fc has no direct effects on the ability of MDA-MB-231 cells to form colonies or proliferate *in vitro* (Figure 3) we investigated its effects on growth of disseminated, dormant, tumour cells in the long bones. MDA-MB-231 cells were injected i.c. in 12-week old BALB/c nude mice that were treated once weekly with either saline (n=14) or 25mg/kg OPG-Fc (n=14) from day 4. Half of the animals in each group underwent either OVX or a sham operation on day 7 (see outline in Figure 4a) as we have previously demonstrated that tumour cells that colonise bones of 12-week old animals have adopted a dormant phenotype at this point (8). As expected, 78.5% of the animals in the OVX/saline group developed long bone tumours by day 35, compared to only 14.5% of the animals in the sham/saline group (Figure 4b,c). Administration of OPG-Fc completely prevented OVX-induced tumour growth, with 7% animals in the OVX/OPG-Fc group having detectable long bone tumours, compared to 78.5% in the OVX/saline group. Tumour frequency in sham-operated animals was unaffected by OPG-Fc (7.5% of animals having detectable bone metastases in sham/OPG-Fc vs 14.5% in sham/saline). In addition, in the small number of animals in which tumours did grow in the bone OPG-Fc significantly reduced tumour size in

both OVX ($P < 0.01$) and sham OVX ($P < 0.01$) operated mice. Luciferase imaging showed no effect of OPG-Fc on tumour grown outside of bone (figure 4d)

This is the first demonstration that administration of OPG-Fc has profound inhibitory effects on disseminated tumour cells *in vivo*, preventing development of overt bone metastases.

OPG-Fc prevents OVX-induced changes to the bone microenvironment

In order to confirm that administration of OPG-Fc reversed OVX-induced bone loss, we carried out a detailed characterisation of the tibia of the animals in the tumour study described in the previous section. As shown in figure 5 a and b, OPG-Fc caused a highly significant increase in bone volume compared to saline control in both the OVX and sham group (percentage of bone volume compared with tissue volume is 11.49 ± 0.51% in saline treated sham operated mice compared with 24.73 ± 1.64% in OPG-Fc treated sham mice ($P<0.001$) and 7.86 ± 0.44% in saline treated OVX mice compared with 23.98 ± 3.22% in OPG-Fc treated OVX mice ($P<0.001$)). The increased bone volume was accompanied by a corresponding decrease in serum TRAP and P1NP levels ($P<0.001$ for sham saline vs. sham OPG-Fc and $P<0.001$ for OVX saline vs. OPG-Fc for both TRAP and P1NP) (figure 5 c and d), confirming that OPG-Fc counteracts OVX-induced bone loss in the animals where growth of disseminated tumour cells was inhibited.

Discussion

In the current study we have used mouse models of MDA-MB-231 breast cancer cell dormancy in bone and advanced *in vivo* imaging to investigate the effects of OVX induced stimulation of osteoclastic bone resorption on the formation of metastases. In addition, we have studied the effects of targeting RANKL-RANK interactions with OPG-Fc on the formation and progression of OVX-induced bone metastases.

We have previously reported that OVX performed 7 days after tumour cell injection of MDA-MB-231 breast cancer cells (i.c) leads to increased bone metastases in 12-week old balb/c mice (8). This result was confirmed in the current study (figure 4). However, our previous studies did not investigate whether this model reflected the clinical situation, in which bone metastases are thought to form from dormant tumour cells. In breast cancer patients it is generally accepted that tumour cells are disseminated in the bone marrow in the early

stages of disease, often before diagnosis, and that these cells remain dormant unless triggered to proliferate as a result of changes in their microenvironment (4-5). In the current study we show that once MDA-MB-231 tumour cells are disseminated in the bones of 12-week old Balb/c mice (with low bone turnover) these tumour cells remain dormant in this environment for the entire 12-week experimental protocol, confirming that our model mimics tumour cell dormancy. A decrease in circulating oestrogen following OVX leads to changes in the bone microenvironment in both humans and animal models (18-20), These changes have the net effect of increasing osteoclastic bone resorption (18-20). Our data confirm significant bone loss in mice following OVX. Importantly we also show that altering the bone microenvironment by OVX stimulates proliferation of tumour cells that have previously been dormant in the bone microenvironment for 8 weeks. OVX stimulation of dormant tumour cells was specific to long bones and no effects were seen in other bones or soft tissues. MDA-MB-231 cells primarily home to long bones following i.c. injection in mice (21) and tumour growth at other sites is uncommon. We therefore hypothesise that lack of detectable tumour growth by luciferase imaging in bones other than long bones following OVX may be due to tumour cells not being disseminated in these sites, this may also be true for lack of tumour growth in soft tissues observed in this model. In the current study only tibiae were harvested for two-photon analysis of disseminated tumour cells and therefore, dissemination at other sites remains to be confirmed. MDA-MB-231 breast cancer cells are oestrogen-independent, whereas the majority of bone metastases occur from oestrogen receptor positive tumours. In an attempt to better reflect bone metastasis from human breast cancer, we carried out pilot studies of tumour cell dormancy in bone using oestrogen-dependent MCF7 cells. In the absence of oestrogen supplementation, these cells did not form bone metastasis following i.c. injection over the subsequent 20 weeks (data not shown). In addition, oestrogen supplementation caused major changes to the bone environment and could not be used in conjunction with OVX (8). We have, therefore, focused this study on oestrogen-independent cells.

Our previous data support that stimulation of disseminated tumour cells in bone to proliferate and form metastases is likely to be driven by osteoclast-mediated mechanisms (8). We have now tested this hypothesis by investigating the effects of inhibiting RANK/RANKL interactions on OVX-induced bone metastases. The binding of RANKL to its cognate receptor RANK is essential for osteoclast maturation, function and survival. The presence of tumour cells in the bone environment stimulates production of RANKL from osteoblasts: *In vitro* co-culture of MDA-MB-231 cells with the human osteoblast cell line

MG-63 results in enhanced production of RANKL (22). Furthermore, MDA-MB-231 cells that do not express RANKL when cultured alone, demonstrate increased RANKL mRNA expression when co-cultured with primary osteoblasts or ST2 osteoblastic cells (23). This increase in RANKL from tumour cells and osteoblasts have the potential to stimulate osteoclastogenesis and drive the formation of osteolytic lesions. Disrupting this interaction via administration of pharmacological RANKL inhibitors including such as RANKL-Fc and OPG-Fc have been show to prevent tumour-associated bone destruction and reduce tumour growth in bone from a variety of tumours including breast, lung, prostate, renal and colon (reviewed in 24). In addition, giving OPG, either simultaneously with or before, tumour cell injection demonstrated that RANKL inhibition significantly delayed de novo formation of MDA-MB-231 breast cancer skeletal metastases (25). Pre-clinical studies show impressive anti-bone metastases effects with RANKL inhibitors and have led to the development of a fully human monoclonal antibody to RANKL (Denosumab) that is currently undergoing a number of clinical trials as a treatment for cancer induced bone disease and to increase bone metastasis-free survival (reviewed in 26 and 27). However, none of the pre-clinical studies have addressed the important clinical question of whether inhibiting RANKL has any effect on dormant tumour cells in the bone microenvironment.

The majority of women who develop bone metastases are post-menopausal and recently published data from clinical trials have shown that treating patients at high risk of developing bone metastases with zoledronic acid is only beneficial to patients who are 5-years or more post-menopausal (28). These data indicate that inhibition of osteoclast activity may have specific anti-tumour effects in a low oestrogen environment. In the current study we mimic the post-menopausal low oestrogen environment by OVX. Our current data support our previous findings that OVX significantly increases osteoclast activity and stimulates proliferation of dormant disseminated tumour cells in bone (8). We now show that these processes are completely inhibited following weekly administration of 25mg/kg OPG-Fc. *In vitro* co-culture studies with breast cancer (MDA-MB-231, MCF7 or T47D) cells and osteoblastic cells indicate that contact with bone can induce expression of RANKL by breast cancer cells and therefore it is possible that inhibiting RANKL may have direct anti-tumour effects on cancer cells growing in the skeleton (29). These findings may in part explain the increased survival benefit seen when treating breast and prostate cancer patients with bone metastases with denosumab compared with zoledronic acid (13).

OPG-Fc is a pharmacologically enhanced native OPG synthesised by Amgen from which the heparin binding domain and the death domain homologous regions have been removed and the remaining amino acids 22-194 OPG peptide have been fused to the Fc domain of human IgG1 (15). The resulting OPG-Fc is a potent as full length OPG but shows a significantly increased circulating half-life. The compound we used is endotoxin free and has been used in multiple published *in vivo* studies (15, 30-36). The doses of OPG-Fc used in animal models of bone metastasis varied considerably depending on the cancer type and duration of the experiment (33-36). We chose to administer 25mg/kg OPG-Fc once per week, as this dose is previously shown to inhibit MDA-MB-231 tumour growth in bone. We confirmed that this treatment regime significantly decreased osteoclastic bone resorption in the mice, resulting in significantly decreased osteoclast and osteoblast activity and almost complete elimination of these cell types on the trabecular and endocortical surfaces of tibiae 4 weeks following commencement of treatment. Interestingly, despite decreased activity of osteoblasts, the growth tibial growth plates were significantly larger in OPG-Fc treated mice compared with control animals, a phenomenon also seen following administration of zoledronic acid (37). Safranin O staining revealed that the enlarged growth plates were made up of proteoglycan with increased numbers of chondrocytes, indicating that inhibition of osteoclast activity is modifying endochondral ossification in this model. However, as the primary goal of this study was to investigate the effects on inhibiting RANK-RANKL interactions on tumour growth in bone, the effects of OPG-Fc on chondrocytes will be the subject of separate investigations.

In conclusion, our study presents the first data showing that disruption of RANK-RANKL interactions following administration of OPG-Fc inhibits growth of dormant tumour cells disseminated in bone *in vivo.* Our data support early intervention with anti-resorptive therapy in a low-oestrogen environment to prevent development of bone metastases.

Acknowledgments

This study was supported by a program grant from Cancer Research UK (to CLE, PIC and IH). PIC is supported by Mrs Janice Gibson and the Ernest Heine Family Foundation. The IVIS Lumina II system was purchased with an equipment grant from Yorkshire Cancer Research. We are grateful for the support from Miss Orla Gallagher and Mr Darren Lath who provided expert bone processing and sectioning.

References

1. Townson JL, Chambers AF. Dormancy of solitary metastatic cells. *Cell Cycle* 2006;**5**:1744-50.

2. Aguirre-Ghiso JA, Bragado P, Sosa MS. Metastasis awakening: targeting dormant cancer. *Nat Med* 2013;**19**:276-7.

3. Chen YC, Sosnoski DM, Mastro AM. Breast cancer metastasis to the bone: mechanisms of bone loss. *Breast Cancer Res* 2010;**12**:215.

4. Clézardin P. (2011) Therapeutic targets for bone metastases in breast cancer. Breast Cancer Res. 13(2):207.

5. Coleman RE, Rathbone E, Brown JE. Management of cancer treatment-induced bone loss. *Nat Rev Rheumatol* 2013;**9**:365-74.

6. Figueroa-Magalhães MC, Miller RS. Bone-modifying agents as adjuvant therapy for early-stage breast cancer. *Oncology (Williston Park)* 2012;**26**:955-62.

7. Coleman RE, Marshall H, Cameron D, Dodwell D, Burkinshaw R, Keane M, et al. Breast cancer adjuvant therapy with zoledronic acid. *N Engl J Med* 2011;**365**:1396-405

8. Ottewell PD, Wang N, Brown HK, Reeves KJ, Fowles CA, Croucher PI, Eaton CL, Holen I. Zoledronic Acid has differential antitumor activity in the pre- and postmenopausal bone microenvironment in vivo. *Clin Cancer Res* 2014;**20**:2922-32.

9. Ottewell PD, Wang N, Meek J, Fowles CA, Croucher PI, Eaton CL, Holen I. (2014) Castration-induced bone loss triggers growth of disseminated prostate cancer cells in bone. End Rel Cancer [EPUB ahead of print]

10. Ottewell PD, Deux B, Monkkonon H, Cross SS, Coleman RE, Clezardin P and Holen I. Differential effect of doxorubicin and zoledronic acid on intraosseous versus extraosseous tumour growth in vivo. *Clin Can Res* 2008;**14**:4658-66.

11. van der Horst G, van den Hoogen C, Buijs JT, Cheung H, Bloys H, Pelger RC, Lorenzon G, Heckmann B, Feyen J, Pujuguet P, Blanque R, Clément-Lacroix P, van der Pluijm G. Targeting of α(v)-integrins in stem/progenitor cells and supportive microenvironment impairs bone metastasis in human prostate cancer. *Neoplasia* 2011;**13**:516-25.

12. Zinonos I, Luo KW, Labrinidis A, Liapis V, Hay S, Panagopoulos V, Denichilo M, Ko CH, Yue GG, Lau CB, Ingman W, Ponomarev V, Atkins GJ, Findlay DM, Zannettino AC, Evdokiou A. Pharmacologic inhibition of bone resorption prevents cancer-induced osteolysis but enhances soft tissue metastasis in a mouse model of osteolytic breast cancer. *Int J Oncol* 2014;**45**:532-40.

13. Lipton A, Fizazi K, Stopeck AT, Henry DH, Brown JE, Yardley DA, Richardson GE, Siena S, Maroto P, Clemens M, Bilynskyy B, Charu V, Beuzeboc P, Rader M, Viniegra M, Saad F, Ke C, Braun A, Jun S. Superiority of denosumab to zoledronic acid for prevention of skeletal-related events: a combined analysis of 3 pivotal, randomised, phase 3 trials. *Eur J Cancer* 2012;**48**(16):3082-92.

14. Zauli G, Melloni E, Capitani S and Secchiero P. Role of full length osteoprotegrin in tumour cell biology. *Cell Mil Life Sci* 2009;**66**;841-815.

15. Morony S, Warmington K, Adamu S, Asuncion F, Geng Z, Grisanti M, Tan HL, Capparelli C, Starnes C, Weimann B, Dunstan CR, Kostenuik PJ. (2005) The inhibition of RANKL causes greater suppression of bone resorption and hypercalcemia compared with bisphosphonates in two models of humoral hypercalcemia of malignancy. Endocrinology. 146(8):3235-43.

16. Ottewell PD, Monkkonen H, Jones M, Lefley DV Coleman RE and Holen I. (2008) Antitumour effects of doxorubicin followed by zoledronic acid in a mouse model of breast cancer. J Natl Cancer Inst. 100:1167-78.

17. Cole AA, Walters LM. Tartrate-resistant acid phosphatase in bone and cartilage following decalcification and cold embedding in plastic. (1987) J Histochem Cytochem. 35:203-6.

18. Mucowski SJ, Mack WJ, Shoupe D, Kono N, Paulson R, Hodis HN. (2014) Effect of prior oophorectomy on changes in bone mineral density and carotid artery intima-media thickness in postmenopausal women. Fertil Steril. 101(4):1117-22.

19. Liu XL, Li CL, Lu WW, Cai WX, Zheng LW. (2014) Skeletal site-specific response to ovariectomy in a rat model: change in bone density and microarchitecture. Clin Oral Implants Res. [EPUB ahead of print]

20. Lee SK, Kadono Y, Okada F, Jacquin C, Koczon-Jaremko B, Gronowicz G, Adams DJ, Aguila HL, Choi Y, Lorenzo JA. (2006) T lymphocyte-deficient mice lose trabecular bone mass with ovariectomy. J Bone Miner Res. 21(11):1704-12.

21. Bellahcene A, Bachelier R, Detry C, Lidereau R, Clezardin P, Castronovo V. (2007) Transcriptome analysis reveals an osteoblast-like phenotype for human osteotropic breast cancer cells. Breast Cancer Research and Treatment. 101:135-148

22. Zhao H, Ning LL, Wang ZY, Li HT, Qiao D, Yao Y, Qin HL. (2014) Calcitonin Gene-Related Peptide Inhibits Osteolytic Factors Induced by Osteoblast In Co-Culture System with Breast Cancer. Cell Biochem Biophys. [Epub ahead of print]

23. Park HR1, Min SK, Cho HD, Kim DH, Shin HS, Park YE. (2003) Expression of osteoprotegerin and RANK ligand in breast cancer bone metastasis. J Korean Med Sci. 18(4):541-6.

24. Roodman GD, Dougall WC. (2008) RANK ligand as a therapeutic target for bone metastases and multiple myeloma. Cancer Treat Rev. 34(1):92-101.

25. Canon JR, Roudier M, Bryant R, Morony S, Stolina M, Kostenuik PJ, Dougall WC. (2008) Inhibition of RANKL blocks skeletal tumor progression and improves survival in a mouse model of breast cancer bone metastasis. Clin Exp Metastasis. 25(2):119-29.

26. Body JJ. (2013) Inhibition of RANK ligand to treat bone metastases. Bull Cancer. 100(11):1207-13.

27. Casas A, Llombart A, Martín M. (2013) Denosumab for the treatment of bone metastases in advanced breast cancer. Breast. 22(5):585-92.

28. Gnant M, Mlineritsch B, Stoeger H, Luschin-Ebengreuth G, Heck D, Menzel C, Jakesz R, Seifert M, Hubalek M, Pristauz G, Bauernhofer T, Eidtmann H, Eiermann W, Steger G, Kwasny W, Dubsky P, Hochreiner G, Forsthuber EP, Fesl C, Greil R; Austrian Breast and Colorectal Cancer Study Group, Vienna, Austria. (2011) Adjuvant endocrine therapy plus zoledronic acid in premenopausal women with early-stage breast cancer: 62-month follow-up from the ABCSG-12 randomised trial. Lancet Oncol. 12(7):631-41

29. Thomas RJ, Guise TA, Yin JJ, Elliott J, Horwood NJ, Martin TJ, Gillespie MT. (1999) Breast cancer cells interact with osteoblasts to support osteoclast formation. Endocrinology. 140(10):4451-8.

30. Miller RE, Jones JC, Tometsko M, Blake ML, Dougall WC. (2014) RANKL inhibition blocks osteolytic lesions and reduces skeletal tumor burden in models of non-small-cell lung cancer bone metastases. J Thorac Oncol. 9(3):345-54.

31. Canon J, Bryant R, Roudier M, Branstetter DG, Dougall WC. (2012) RANKL inhibition combined with tamoxifen treatment increases anti-tumor efficacy and prevents tumor-induced bone destruction in an estrogen receptor-positive breast cancer bone metastasis model. Breast Cancer Res Treat. 135(3):771-80.

32. Canon J, Bryant R, Roudier M, Osgood T, Jones J, Miller R, Coxon A, Radinsky R, Dougall WC. (2010) Inhibition of RANKL increases the anti-tumor effect of the EGFR inhibitor panitumumab in a murine model of bone metastasis. Bone. 46(6):1613-9.

33. Zauli G, Melloni E, Capitani S, Secchiero P. (2009) Role of full-length osteoprotegerin in tumor cell biology. Cell Mol Life Sci. 66(5):841-51.

34. Armstrong AP, Miller RE, Jones JC, Zhang J, Keller ET, Dougall WC. (2008) RANKL acts directly on RANK-expressing prostate tumor cells and mediates migration and expression of tumor metastasis genes. Prostate. 68(1):92-104.

35. Vanderkerken K, De Leenheer E, Shipman C, Asosingh K, Willems A, Van Camp B, Croucher P. (2003) Recombinant osteoprotegerin decreases tumor burden and increases survival in a murine model of multiple myeloma. Cancer Res. 63(2):287-9.

36. Morony S, Capparelli C, Sarosi I, Lacey DL, Dunstan CR, Kostenuik PJ. (2001) Osteoprotegerin inhibits osteolysis and decreases skeletal tumor burden in syngeneic and nude mouse models of experimental bone metastasis. Cancer Res. 61(11):4432-6.

37. Haider M-T, Holen I, Hunter K, Brown HK (2014) Modifying the osteoblastic niche with zoledronic acid in vivo - potential implications for breast cancer bone metastasis Bone. 66:240-50

Figure legends

Figure 1. Effects of ovariectomy on proliferation of MDA-MB-231 breast cancer cells in bone following long-term dormancy. Panel a) is a diagrammatic representation of the protocol. Panel b) presents photographs of luciferase expressing MDA-MB-231 cells growing in female BALB/c nude mice 84 days following tumour cell injection and 28 days following ovariectomy or sham operation. Percentage of mice with tumours growing in bone and soft tissue on day 56 (at ovariectomy) and after ovariectomy are show in in panel c. Panel d shows dormant MDA-MB-231 cells in mouse tibia 56 days after tumour cell injection and panel e shows the effect of ovariectomy on bone volume 28 days following operation.

Figure 2. Effects of OPG-Fc on mouse long bone. Female BALB/c nude mice were treated with 25mg/kg OPG-Fc or 0.1ml of 0.2% saline 1x per week for 4 weeks, panel a) shows histological sections following Goldner's staining (bone shown in green), Safranin O staining (non-ossified bone shown in red) and TRAP staining (osteoclasts can be identified as large, pink, multinucleated cells lining the bone surface and osteoblasts are highlighted with black arrows). µCT images showing bone architecture are shown in panel b) and panel c) is a graph showing the effects of OPG-Fc on bone volume compared with trabecular volume ± SEM.

ELISA analysis of serum TRAP (units per litre) and P1NP (ng/ml) ± SEM are shown in panels d) and e) respectively. * = p<0.01, *** = p<0.0001.

Figure 3. Effects of OPG-Fc on growth of MDA-MB-231 tumour cells *in vitro.* Line graphs showing effects of increasing concentration of OPG-Fc on growth of MDA-MB-231 tumour cells in media supplemented with 10% FCS a) and reduced serum concentration on growth of MDA-MB-231 tumour cells treated with saline or 100g/ml OPG-Fc b) for up to 6 days in culture. Panel c) shows effects of increasing concentrations of OPG-Fc on ability of MDA-MB-231 cells to form colonies on plastic. Data presented as mean ± SEM.

Figure 4. Effects of OPG-Fc on ovariectomy-induced tumour growth in bone. Panel a) is a diagrammatic representation of the experimental protocol. Panel b) presents photographs of luciferase expressing MDA-MB-231 cells growing in female BALB/c nude mice 31 days following injection of saline or OPG-Fc and 28 days following ovariectomy or sham operation. Panel c) shows the percentage of mice with tumours in bone and outside of bone (lungs and eye socket) at the end of the experiment and panel d) shows mean bioluminescence per tumour in bone and outside of bone ± SEM. *** = p<0.0001. Panel e) shows photomicrographs of H&E stained histological sections from the left tibiae of BALB/c nude mice 31 day following injection of saline or OPG-Fc and 28 days following ovariectomy or sham operation, tumour circumference in bone is highlighted in blue.

Figure 5. Effects of OPG-Fc on ovariectomy-induced bone loss in the tibia. Panel a) shows cross sectional and longitudinal images of female BALB/c mouse tibiae following 4 weekly injections of saline (control) or 25mg/kg OPG-Fc and 28 days following either sham operation or ovariectomy. Panel b) shows trabecular volume compared with bone volume for these mice and panels c) and d) show ELISA analysis of serum TRAP (units per litre) and P1NP (ng/ml) ± SEM respectively. *** = P < 0.0001

Figure 1

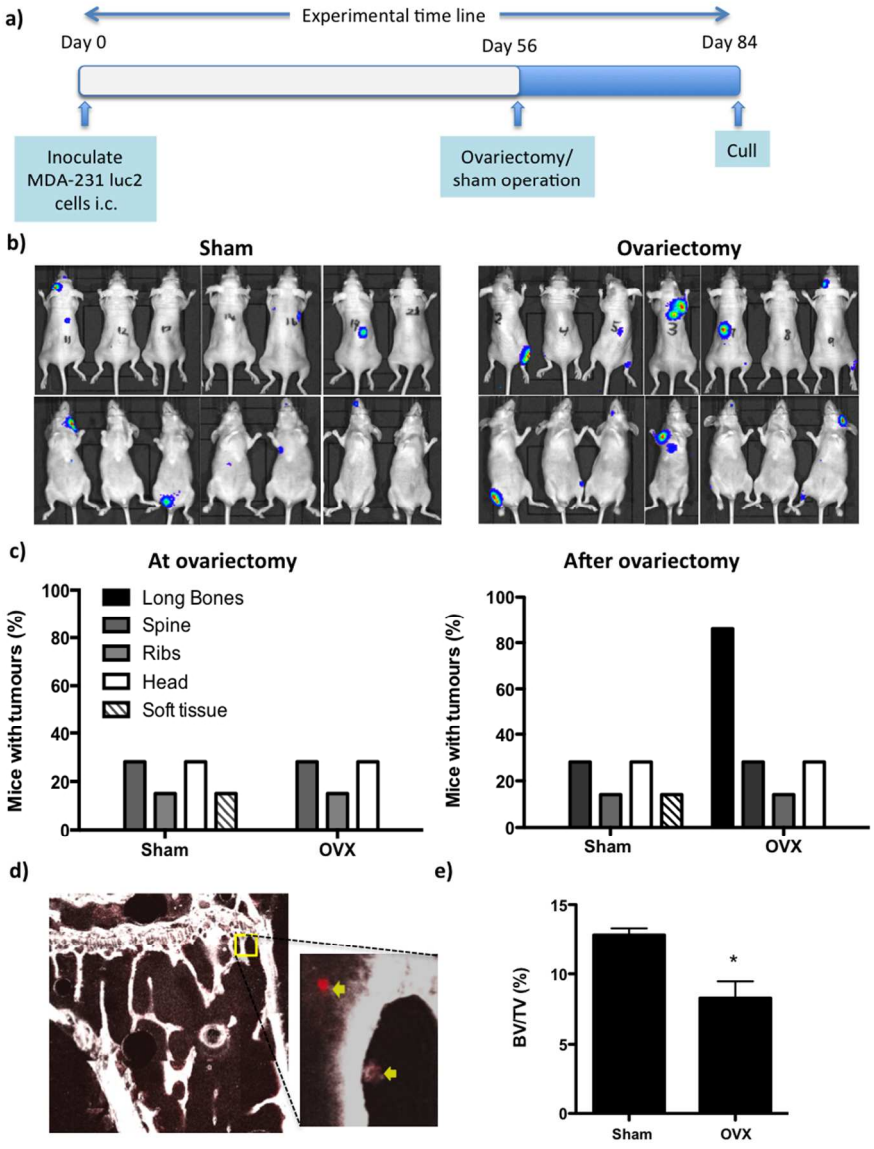

352x470mm (72 x 72 DPI)

Figure 2

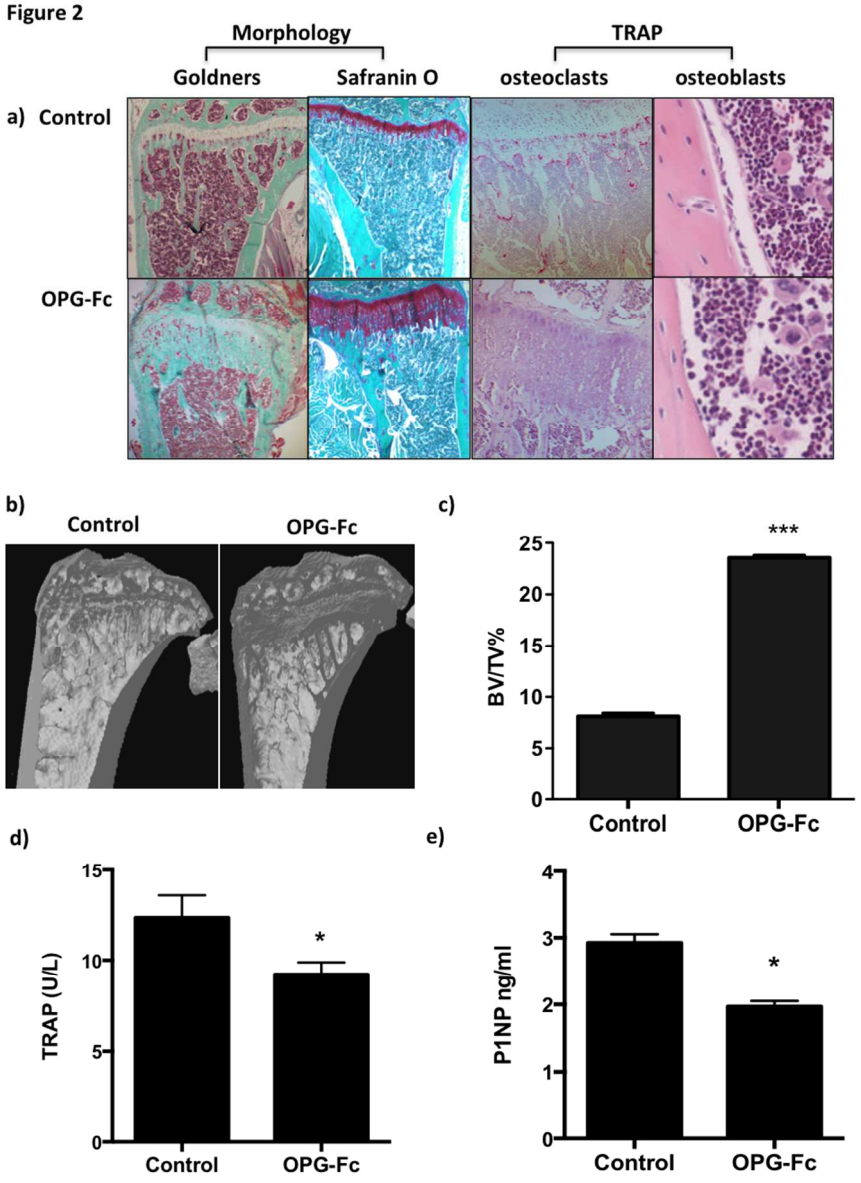

352x470mm (72 x 72 DPI)

Figure 3

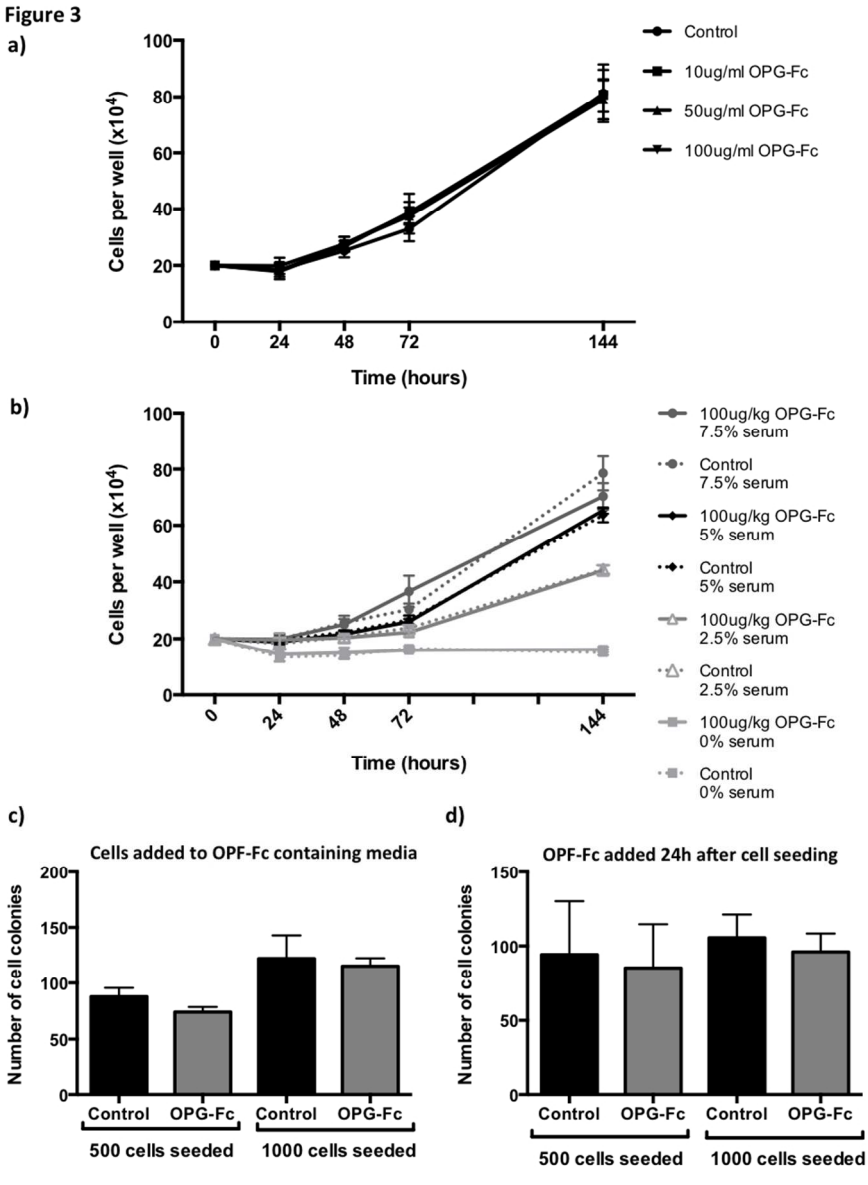

352x470mm (72 x 72 DPI)

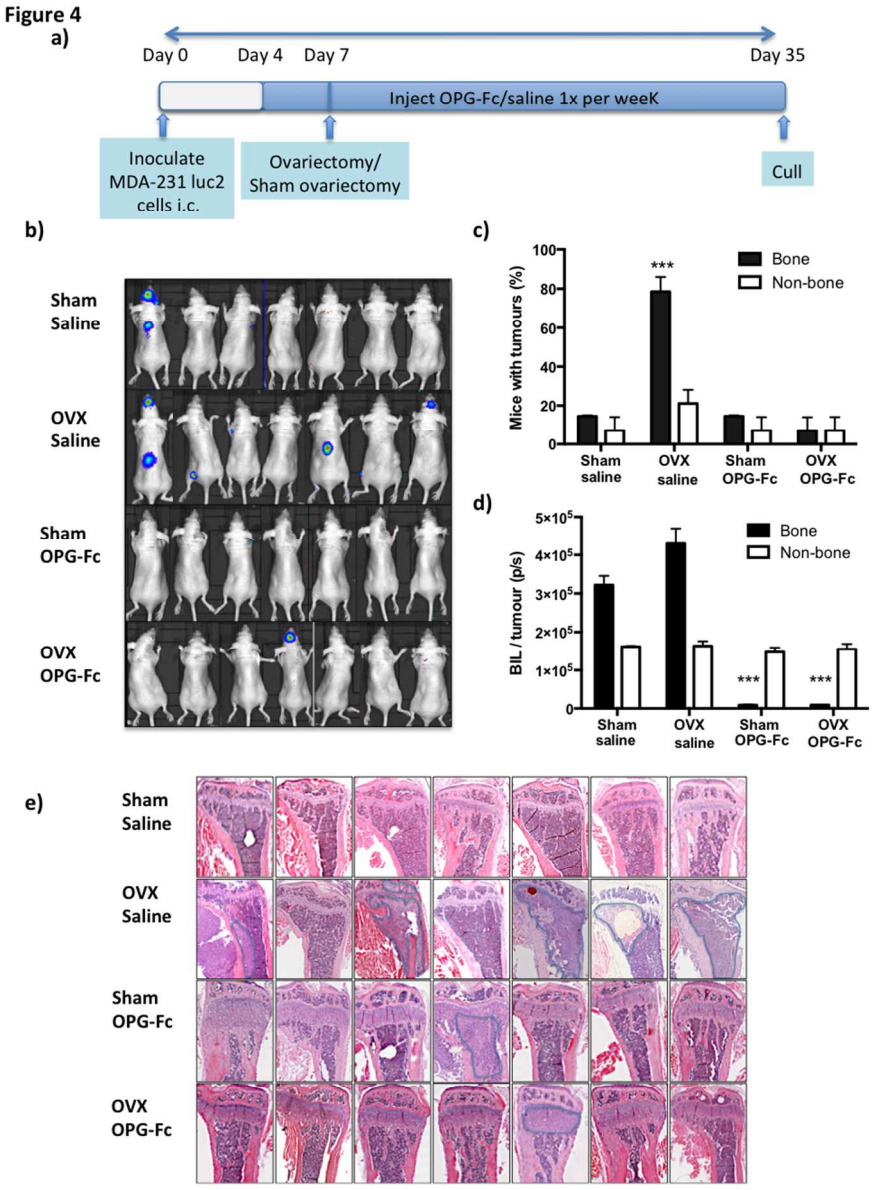

352x470mm (72 x 72 DPI)

Figure 5

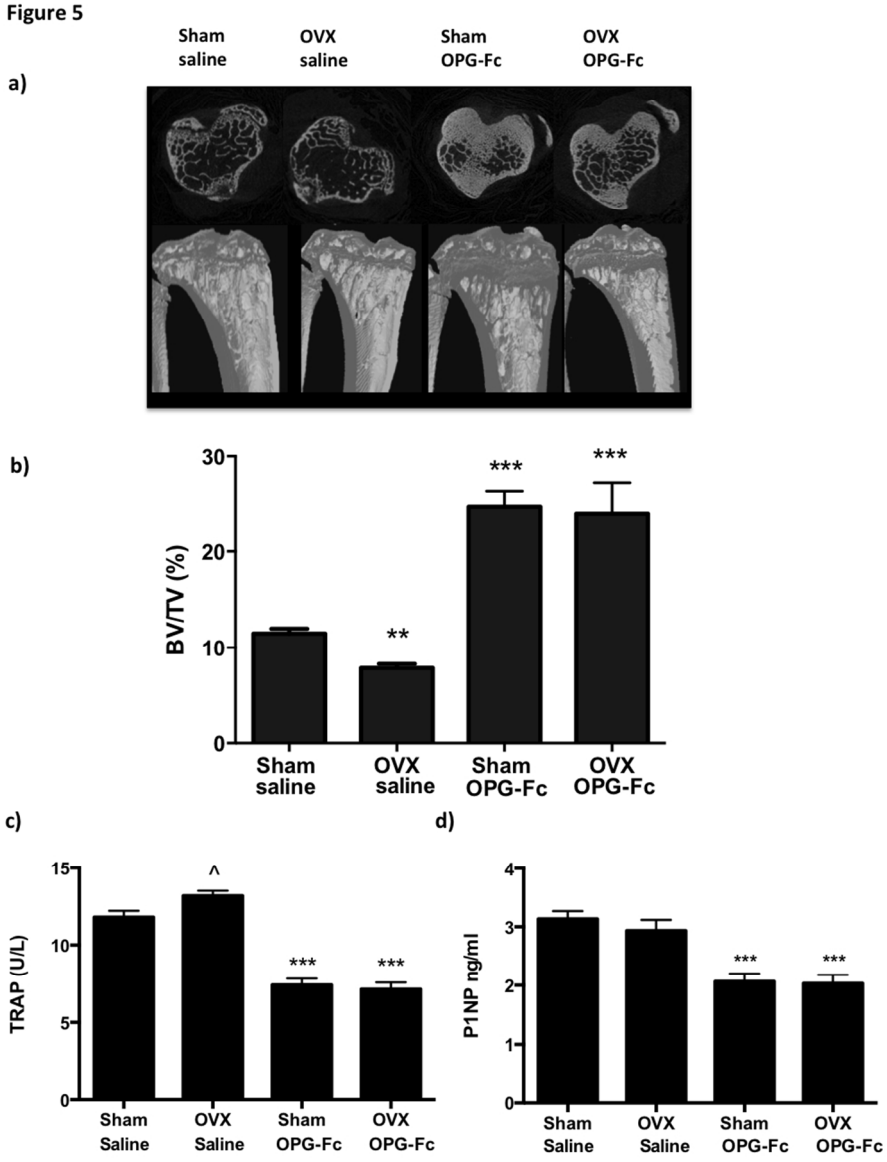

352x470mm (72 x 72 DPI)